Lab on a Chip

Cite this: *Lab Chip*, 2012, **12**, 3514–3520

www.rsc.org/loc

PAPER

Novel technologies for the formation of 2-D and 3-D droplet interface bilayer networks†

Yuval Elani,[ab] Andrew J. deMello,[c] Xize Niu[d] and Oscar Ces*[ab]

Received 23rd March 2012, Accepted 16th July 2012
DOI: 10.1039/c2lc40287d

Droplet interface bilayer (DIB) networks have vast potential in the field of membrane biophysics, synthetic biology, and functional bio-electronics. However a technological bottleneck exists in network fabrication: existing methods are limited in terms of their automation, throughput, versatility, and ability to form well-defined 3-D networks. We have developed a series of novel and low-cost methodologies which address these limitations. The first involves building DIB networks around the contours of a microfluidic chip. The second uses flow rate and droplet size control to influence droplet packing geometries within a microfluidic chamber. The latter method enables the controlled formation of various 3-D network arrays consisting of thousands of interconnected symmetric and asymmetric lipid bilayers for the first time. Both approaches allow individual droplet position and composition to be controlled, paving the way for complex on-chip functional network synthesis.

Introduction

The past decade has seen the development of a new type of model membrane system, the droplet interface bilayer (DIB).[1] The physical principle underpinning DIB formation is simple: when two lipid monolayer-encased water-in-oil droplets are brought together, oil is excluded from the interface and a lipid bilayer results (Fig. 1). DIBs have several inherent features which give them a significant advantage over other more traditional model membrane systems such as supported lipid bilayers, black lipid membranes, and liposomes. Amongst these are their high temporal and mechanical stability,[2] the absence of an interfering solid support, the ability to directly form asymmetric bilayers,[3] and the possibility for electrode insertion into the droplets for electrical measurements.[4] DIBs are also amenable to lab-on-a-chip applications where they have the potential to be used as biosensors, in medicinal diagnostics, and for screening ion-channel blockers.[5]

However, perhaps the most useful characteristic of DIBs is their ability to form interconnected bilayer networks, achieved by joining three or more droplets together. This feature is unique to DIBs and has been exploited in a number of studies. By incorporating natural and engineered proteins, DIB networks have been designed to act as simple functional electronic circuits.[6] Additionally, networks capable of sensing light and acting as bio-batteries and light sensors have been created.[5] A modified setup where DIBs are enclosed in oil-in-water droplets has recently been shown to function in aqueous environments, a development which expands its applications to the domain of responsive therapeutics.[7]

However, to extend the functionalities and applications of DIB networks to a new level, automated methods for creating extensive networks of pre-defined architectures need to be developed. Importantly, control over individual droplet position and composition must be achieved to afford the desired functionality to the network. We report herein the use of droplet based microfluidic devices which address these issues. By

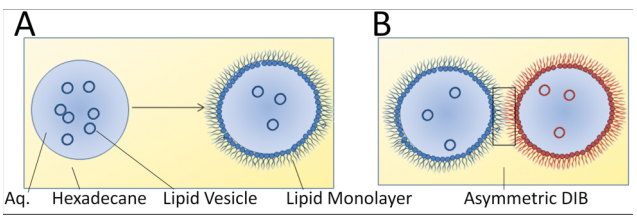

Fig. 1 The 'lipid-in' approach of forming DIBs entails having lipid vesicles inside the aqueous solution. **(A)** Vesicles rupture at the oil/aqueous interface and a monolayer forms around the droplet, with the hydrophobic fatty acid tails facing the oil and the hydrophilic headgroup facing the aqueous solutions. **(B)** By having vesicles of different composition in the two droplets, asymmetric bilayers (where the constituent leaflets of the bilayers have differing lipid compositions) can be formed.

[a]*Department of Chemistry, Imperial College London, Exhibition Road South Kensington, London, UK, SW7 2AZ. E-mail: o.ces@imperial.ac.uk*
[b]*Institute of Chemical Biology, Imperial College London, Exhibition Road, South Kensington, London, UK, SW7 2AZ*
[c]*Institute for Chemical and Bioengineering, Department of Chemistry and Applied Biosciences, ETH Zurich, Switzerland*
[d]*Engineering and the Environment, and Institute for Life Sciences, University of Southampton, Highfield, Southampton, UK, SO17 1BJ*
† Electronic supplementary information (ESI) available: details of experimental setup and video of DIB array formation. See DOI: 10.1039/c2lc40287d

building on previous work,[8] DIB networks of pre-defined architectures, as well as long range 2-D and 3-D DIB arrays have been created.

The most basic and extensively used approach to DIB formation involves manual micropipetting of aqueous droplets, and their subsequent movement using a micro-manipulator.[5] This approach is attractive in its simplicity, but the size of the networks formed *via* this method is limited—due to a lack of automation—to tens of bilayers. Additionally, the nature of the droplet manipulation technique prohibits 3-D network formation, as there is no confinement in the vertical direction due to the need for micromanipulator access from above.

There have also been several successful attempts at translating DIB platforms into microfluidic formats. DIBs have been formed using cross-channels to bring aqueous compartments into contact,[9] using dielectrophoresis and electrowetting-on-dielectric methods to manipulate droplets,[10,11] and by employing approaches based on oil extraction into polydimethylsiloxane (PDMS).[12] Microfluidic methods such as these have several advantages, including low sample volumes, fine control over bilayer area, as well as having dimensions similar to cellular systems (*ca.* 50–100 μm).[13] In addition, the controlled manner in which droplets are brought together in microfluidic systems means that droplets are more resilient to merging. However, these methods also have limitations. The primary limitation is that a maximum of only two bilayers can be produced in sequence, thus prohibiting DIB network formation. This is in contrast to the micropipetting method which forms networks of tens of bilayers, and the microdroplet approach which forms networks of hundreds of bilayers. Secondary limitations of these microfluidic methods include the diminished temporal stability of the DIBs, the inability to vary bilayer area (determined by droplet size) without reconfiguration of the equipment, and the fact that the DIBs may not be stable with lipid compositions other than the robust, but less biologically relevant 1,2-diphytanoyl-sn-*glycero*-3-phosphocholine (DPhPC) lipid.

Previous work from our laboratory has shown the potential of a microdroplet approach to DIB formation.[8] This method is capable of creating extensive DIB networks *via* high-throughput generation of microdroplets. In addition, an extensive 3-D DIB array was constructed for first time. However the precise packing of the droplets was undefined, and could not be controlled or directed to give different network geometries. In addition, the device was based around a glass capillary which hampered network imaging, and lacked the versatility of PDMS with respect of lab-on-chip applications. Finally, it was not capable of directing droplets of set compositions to lie at specific points in a network.

In summary, microfluidic methods of forming extensive DIB networks are necessary but are, as of yet, lacking. Herein, we describe two microfluidic devices capable of forming extensive 2-D and 3-D interconnected DIB networks on-chip, in an automated and high-throughput fashion. The first device demonstrates for the first time the ability to form networks of predefined architectures using the contours of microfluidic circuits as templates around which the network forms. The second device incorporates a linear channel in which several extensive 2-D and 3-D DIB arrays can be formed in a controlled manner. In the latter case, network geometry is directed using the droplet size and flow rate. Significantly, this is the first time that 3-D DIB networks have been formed in a controlled and well-defined way. In both devices, control over droplet position and bilayer composition within the resulting networks is achieved.

Results and discussion

All DIBs were formed using the 'lipid-in' approach.[3] Three types of droplets which differed in their lipid compositions were used. The first droplet type contained DPhPC lipid. The second droplet type contained 1,2-dioleoyl-sn-*glycero*-3-phosphocholine (DOPC), with 0.1 mol% 1,2-dioleoyl-sn-*glycero*-3- phosphoethanolamine-*N*-(7-nitro-2-1,3-benzoxadiazol-4-yl (NBD-PE). The third droplet type contained equal amounts of 1,2-dipalmitoyl-sn-*glycero*-3-phosphocholine (DPPC) and DPhPC with 0.1 mol% 1,2-dioleoyl-sn-*glycero*-3-phosphoethanolamine-*N*-(lissamine rhodamine B sulfonyl) (ammonium salt) (Rh-PE). Fluorescently-tagged lipid was present in the latter two droplet types to allow visualisation using fluorescence microscopy.

Device one: junction network device

The DIB junction network was formed using the device outlined in Fig. 2. Droplets entered at the 'trunk' of the device with syringes attached to the two branches. These were attached to a programmable syringe pump, whose settings allowed the droplets to be directed to the different parts of the network *via* hydraulic pressure differences. 40 pL droplets were produced off-chip according to droplet manufacturing protocols described previously.[8] Briefly, the syringe pump connected to the branch of interest was operated under refill mode as shown in Fig. 2. On the other end of the device, a thin wall PTFE tubing was fixed to homemade robotic head actuated with a solenoid. The tip of the tubing was moved alternately into oil and vesicle solutions. The retention times of the tip in each phase were adjusted with a homemade Labview© program, to ensure a stream of droplets could be generated with the right droplet size, spacing and sequence.

These droplets were then introduced from tubing into the main trunk of the channel at 1 μL min^{-1} where they formed a linear DIB sequence. When the droplets reached the 'junction-point' (the central area which lies at the junction of the three branches, see Fig. 2) they were directed to one of the two downstream branches using the syringe pump settings, with droplets travelling down whatever branch was under suction at the time. If the same syringe was left under suction, the droplets continued to arrange linearly down that specific branch. In order to change the path direction of droplets to the adjacent branch, the syringe modes were reversed: the previously refilling syringe was stopped, and the previously stationary syringe was set to operate under suction at 1 μL min^{-1}. Fig. 3 illustrates this process.

Junction network – discussion

Using the junction network device, it was possible to form a 2-D DIB network of a predefined architecture according to the contours of the microfluidic chip (Fig. 4). Additionally, the positioning of individual droplets within the network could be controlled with hydraulic pressures. This allowed distinct DIB

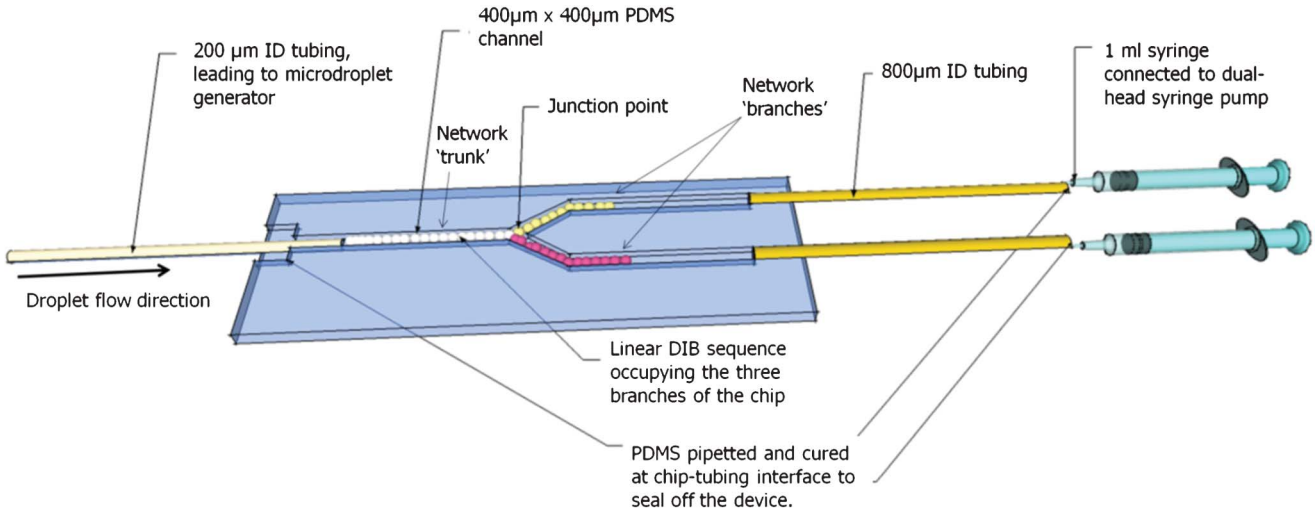

Fig. 2 Schematic of the 'branched' junction network microfluidic device, showing its major features.

sequences to be formed in each of the three branches of the network.

In the simplest scenario it was possible to create a branched network of DPhPC DIBs (Fig. 4A). The DIB sequences in each of the three branches could also be controlled. For instance, it was possible to create sequences of symmetrical bilayers of DOPC, DPhPC, and DPPC, with each DIB sequence occupying a different branch of the chip (Fig. 4B). Finally, the approach was robust enough to allow the formation of asymmetric DIB sequences, and was also able to control the position and composition of individual droplets within the networks. This is exemplified by having an individual droplet of a different composition to all other droplets present lying at the 'junction-point' that connects the different sequences in the three branches together (Fig. 4C).

This device relies on individual droplets being fully contained by the channel walls. As such, droplets deform to conform to the channel geometry. This in turn influences the bilayer area, which is maximised to fit the cross sectional area of the channel.

The experimental set-up could be extended to the generation of more complex 2-D networks, directed by different chip architectures, and specifically tailored for the experiment to be performed. To achieve this, three key criteria must be met. First,

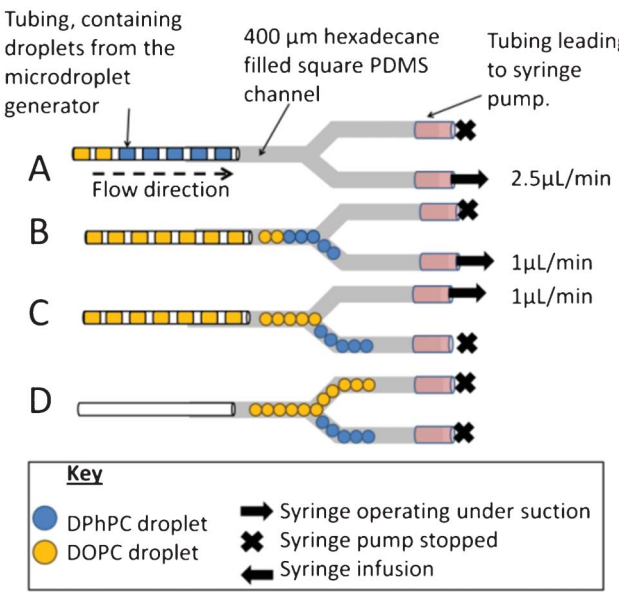

Fig. 3 Illustration of the different stages involved in the formation of a branched DIB network. **(A)** Droplets are generated with one syringe operating under suction, the other being stationary. **(B)** Droplets enter the channel and make contact with one another resulting in a linear DIB sequence. When this sequence reaches the junction-point, the droplets travel down the path that is under suction. **(C)** To change the path down which droplets travel, the flow-settings of the two syringe pumps are reversed: the previously stationary syringe is changed to operate under suction and *vice versa*. If droplets positioned themselves in an undesired channel, they were repositioned using pressure bursts (see ESI†). **(D)** Once the desired network is created, all the pumps are stopped.

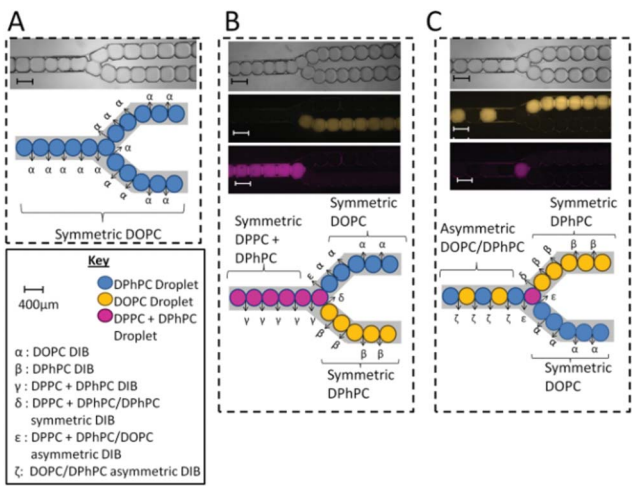

Fig. 4 Examples of the branched networks that were created, with branches containing DIB sequences of different compositions. **(A)** Branched network of same-composition DIBs. **(B)** Network where each of the branches contained DIB sequences of different lipid compositions. **(C)** Network containing an asymmetric DIB sequence in one of its branches, and an individual distinct droplet directed to lie in the network 'junction-point' connecting the constituent branches. Scale bar = 400 μm.

the dimensions of the droplets must be similar to those of the channels. This is necessary to achieve droplet confinement, thus allowing the DIB sequence to follow the chip architecture. Second, microfluidic control over the position of individual droplets needs to be achieved for the droplets to adopt the desired position in the network (in our case this was achieved using hydraulic pressure differences). Finally, the droplet lipid composition must yield DIBs that are stable enough to withstand the surface tension imbalances which lead to droplet coalescence.[14]

Device two: linear channel device for the formation of 2-D and 3-D DIB arrays

A cylindrical linear channel device was used to create and contain long-range 2-D and 3-D DIB arrays (Fig. 5). Unlike the branched network device, the droplet diameters were smaller than that of the channel (400 μm). As a result they were not fully constrained by the channel, and were capable of stacking in two and three dimensions to form interconnected DIB arrays (a review of self-assembled droplet arrays can be found elsewhere).[15] By varying the droplet size and flow rate, four distinct droplet packing geometries—and hence distinct DIB network array architectures—were produced. These are referred to here as the one-, two-, three- and four-row arrangements (see Fig. 6 and video in ESI†). The interplay between such parameters and droplet packing arrangement has been experimentally characterised in a recent study which relates to the field of 'liquid-crystallography'.[16]

Higher packing geometries were favoured both by smaller droplet sizes and by higher flow rates. With smaller diameters, more droplets could fit in a unit volume (in both two and three dimensions) before experiencing a packing frustration which drives them to spread out and move along the length of the channel. Similarly, as the rate at which droplets entered the channels was increased, droplets had less time to rearrange along the length of the channel to alleviate the packing frustration before the next droplet arrived. This resulted in droplets arranging themselves both above and to the side of previously present droplets, resulting in higher packing geometries. These effects can be seen in the ESI video.†

Droplets of different sizes, ranging from 14 pL to 180 pL were generated off-chip and introduced into the device at a flow rate

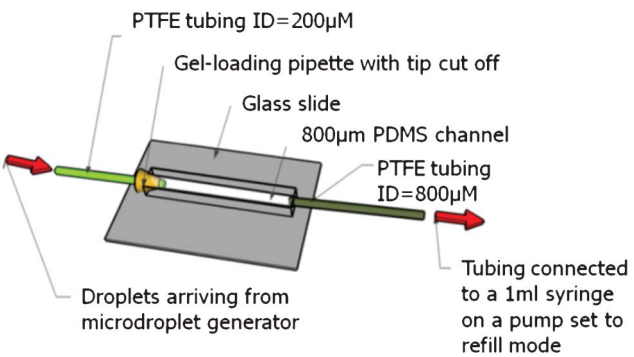

Fig. 5 Schematic of the 'linear channel device'. Long range 2-D and 3-D array networks of DIBs form within the channel. Network architectures are determined both by the droplet size and the flow rate.

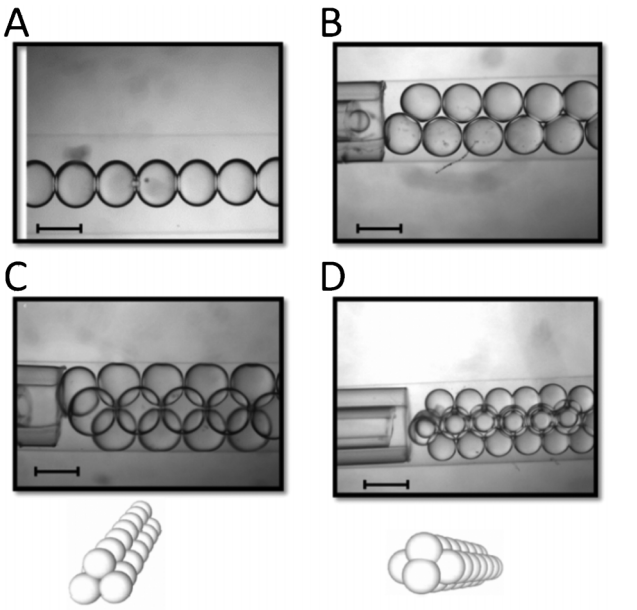

Fig. 6 The four DIB array networks that were produced **(A)** Linear DIB array of sequential bilayers. **(B)** Two-row DIB network. **(C)** Three-row DIB array network, together with a schematic of the 3-D packing arrangement that the droplets adopt. **(D)** Four-row DIB array network together with a schematic of the 3-D packing arrangements that the droplets adopt. Scale bar = 400 μm.

of between 0.2 and 2 μL min^{-1}, depending on the desired packing arrangement. On entering the microfluidic channels droplets made contact and DIBs were formed. All DIBs were symmetric, and were composed of DPhPC lipid, unless mentioned otherwise. It is worth noting that all four packing arrangements had significant long range order, which lasted throughout the channel length (approximately 30 mm long). Furthermore, the networks were temporally stable, with no change in packing arrangement or droplet merging events observed over a 36 h period. Finally, once the DIB arrays were formed, they retained their integrity even when the flow was suddenly stopped; pressure was not needed to maintain the droplet packing arrangements.

One-row arrangement. A simple linear arrangement of DIBs (corresponding to a network of sequential bilayers) was formed with 61 nL droplets and an outflow rate of 1 μL min^{-1} (Fig. 6A). Once the droplets departed into the channel, they remained adjacent to the tubing and did not move with the general flow of the oil. This is thought to be because they were residing on the channel floor, which provided a force resisting motion; the oil phase therefore flowed around the stationary droplet. When the next droplet arrived the previously stationary droplets were pushed along the channel, and a new DIB formed soon after contact was made.

Two-row arrangement. With smaller droplets (21 nL) and higher outflow rates (1.5 μL min^{-1}) an ordered 2-D arrangement of two parallel rows of droplets was produced, with one row being displaced a distance of half a droplet diameter relative to the second row (Fig. 6B).

Three-row arrangement. At higher flow rates (2 μL min^{-1}) with 21 nL droplets, a third packing geometry—this time involving 3-D arrangement of droplets where droplets start arranging themselves in the vertical direction—is observed. This arrangement consists of two rows of droplets lying next to each other, above which is a third row, displaced a distance of half a droplet diameter relative to the two rows lying beneath it (Fig. 6C). This is akin to a portion of a hexagonal close packed face centred cubic (fcc(111)) lattice.

Under conditions of defined flow rate and droplet size, a 'two-row' arrangement initially forms. However the faster outflow rate leaves less time for the droplets to move outward along the channel before the next droplet arrives. Because of this the channel became increasingly packed, and incoming droplets were forced to enter into a third row above the plane of the first two rows (see video in ESI†).

Four-row arrangement. A reduction in droplet size (11 nL) coupled with an outflow rate of 2 μL min^{-1} generates a 3-D geometry consisting of four parallel rows of droplets: two rows in the microscope plane which are not in contact with one another, and two rows lying above and below these, which are in contact with one another (Fig. 6D). This can be described as a portion of a square close packed face centred cubic (fcc(100)) lattice.

Linear channel device—discussion

The above approach was robust in producing distinct regular repeating networks of DIBs. The device allowed extensive and distinct 1-D, 2-D and 3-D DIB networks to be formed simply by varying droplet size and outflow rate. Network architecture could thus be directed using external parameters with the same design specifications. Droplet size—and by extension bilayer area—of the DIBs in the networks was uniform, with all droplet cross sectional areas within 3% of the average. The networks were produced in a high-throughput manner, which is exemplified by the four-row arrangement. Here, an interconnected network comprising of 1600 DIBs was formed in the space of 30 minutes (a DIB formation rate of approximately 0.9 Hz). Finally, the method is fully automated. Once the flow rate and droplet size parameters are defined, no additional inputs are needed. To achieve similar results using micro-injection methods would require the injection of thousands of droplets individually. The impracticality of this limits the networks formed using such techniques.

Due to the fact that the one- and two-row arrangements were generated in an ordered and predictable manner, it was possible to direct droplets of user-defined compositions to distinct locations within the networks by control of the sampling order. This allowed compositional arrays of symmetric and asymmetric DIBs to be generated.

In the case of the linear arrangement, a DIB sequence of asymmetric DPhPC/DOPC bilayers was formed with droplets in the order $(ABAB)_n$ where A and B are droplets of different lipid compositions (Fig. 7A). An introduction of a third lipid type, DPPC allowed more complex sequences to be made (Fig. 7B). The device is versatile enough to form droplets in any order, thus making it possible to generate a wide range of membrane sequences. The same concept was applied to the two-row architecture to form distinct compositional patterns (Fig. 7C–F). When droplets were formed in an $(ABAB)_n$ sequence, they arranged themselves so that one of the two rows contained only droplet type A, and the parallel row contained only droplet type B. By sampling droplets in different sequences, other user-defined patterns were constructed. In each of these cases the

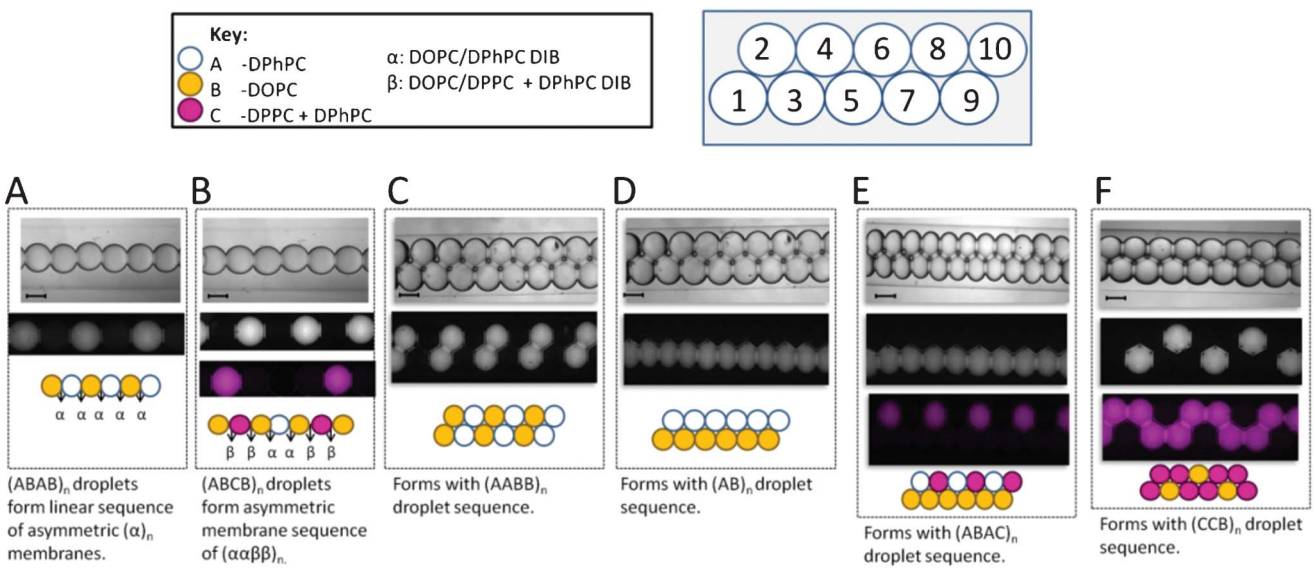

Fig. 7 Examples of the compositional patterned arrays that were introduced into the networks. **(A)** Asymmetric sequences of DIBs formed using alternating droplets of two different lipid compositions. **(B)** Droplets of three different compositions produce more complex membrane sequences. **(C,D,E,F)** The regular and predictable assembly of droplets in the two row arrangement (inset) allowed distinct DIB patterns to be generated. The inset figure shows the relative order in which droplets enter the channel. The regular and predictable manner in which the droplets assembled once entering the channel allowed the patterned arrays to be generated simply by sampling droplets in different orders, leading to the creation of any desired pattern. Scale bar = 400 μm.

droplets had different numbers of symmetric/asymmetric bilayers associated with them.

Multi-contact DIBs

Droplets in each of the networks formed using the described device have a different number of DIBs associated with them. It is possible to form arrangements where droplets have n DIBs associated with them, where n = 1–7, as demonstrated in Fig. 8A. This contrasts with previous reports of microdroplet DIB formation which allow the formation of n = 2 sequences, as well as an undefined multi-contact DIB arrangement.[8] The micro-injection technique used by others to create DIB networks allows a maximum of n = 4 DIBs per droplet, with droplets being arranged in two dimensions only.

As shown in Fig. 8A, central droplets in each arrangement have a set number of satellite droplets associated with them *via* a bilayer. Controlling the composition of individual droplets within the networks allows the satellite droplets to contain specific lipids/protein/drugs: the effects that these variables have on a process contained in a central droplet can be directly compared. Processes such as drug diffusion rates and protein activity could thus be measured in competition with one another (indeed, a first step towards this has already been made, with the measurement of fluorescent molecule diffusion kinetics through droplet interface surfactant bilayers).[17]

Experimental

Lipid preparation

All lipids were purchased from Avanti Polar Lipids as powders. Three different lipid vesicle solutions were made up: DPhPC; DOPC with 0.1% NBD PE; and 49.95% DPhPC, 49.95% DPPC with 0.1% Rh-PE. Lipid powder was dissolved in chloroform, which was subsequently removed under a nitrogen stream, with the resultant lipid film being lyophilised overnight. The film was then hydrated with 10 mM HEPES solution (4-(2-hydroxyethyl)-1-piperazineethanesulfonic acid) (Sigma Aldrich) at pH 7.4 to yield a 10 mg ml^{-1} lipid solution. The solution was then agitated using a vortexer, put through five freeze–thaw cycles, and extruded 21 times through a polycarbonate membrane of 100 nm pore size (Avanti Polar Lipids) to give 100 nm diameter vesicles. These solutions, together with hexadecane (99%, Sigma Aldrich) were used to form the water-in-oil droplets.

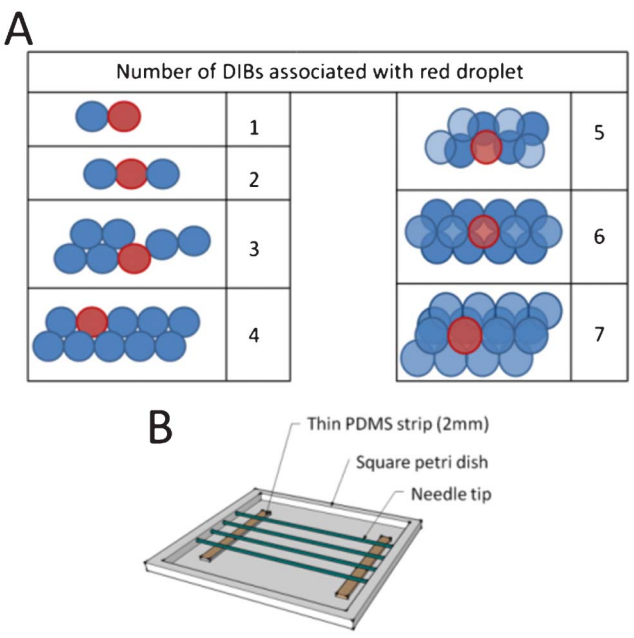

Fig. 8 **(A)** The linear channel device was able to produce droplets with n associated DIBs, where n = 1–7. **(B)** The hollow channel of the 'linear channel device' was formed using needle tips as a mould around which PDMS is cast. A thin PDMS strip raised the needles above the petri-dish surface which was then filled with uncured PDMS.

PDMS preparation

PDMS substrates were prepared using Sylgard 184 Silicone Elastomer Kit (Dow Corning). A 1 : 10 ratio of curing agent to bulk elastomer was mixed thoroughly, degassed, poured onto the masks, and left to cure overnight at room temperature

Junction network device fabrication

The junction network chip photo-mask was designed using AutoCAD (AutoDesk). The designs were sent to JD Photo-Tools (Photodata Test Services Ltd, Oldham) for development under a darkfield polarity. The chip features were microfabricated silicon wafers (IDB Technologies Ltd. Whitley, UK) using standard soft lithography techniques. SU-8 50 (Chestech Ltd. Rugby, UK) was used as the master photoresist and was deposited to a thickness of 400 μm, which defined the eventual thickness of the channel. Microposit EC-Solvent (Chestech Ltd. Rugby, UK) was used to remove unexposed resist, and isopropylalcohol and distilled water were used for rinsing the substrate.

200 μm ID tubing was threaded through the 'trunk' of the branched network. Two pieces of 800 μm ID tubing were pushed into the two 'branches' of the network. The system was then sealed by placing the chip on a hotplate at 120°, and pipetting drops of pre-prepared PDMS at the tubing-chip interface. The PDMS—which cures within 20 s at this temperature—acts as a glue which seals the system. The chip, syringes, and tubing were completely filled with hexadecane, and all air bubbles were expelled from the system.

Linear channel device fabrication

This device was fabricated using a hypodermic needle tip (21G, 800 μm outer diameter, 120 mm length, Sterican, B Braun, Germany) as a cast around which PDMS cured. The needle tips were placed on a raised strip of PDMS (2 mm thickness) in a square petri-dish (100 mm, VWR, UK), and PDMS mixture was poured into the container until the needles were fully submerged (see Fig. 8B). After curing, the needle tips were removed leaving a hollow 800 μm diameter channel.

The rest of the device was fashioned around this hollow channel. 200 μm ID tubing was threaded through a gel-loading pipette tip (Cole-Parmer, UK), until the tubing could not be pushed any further due to the decreasing diameter of the tip. The pipette was then cut at this point, and pushed into the channel until a tight fit was achieved. 800 μm ID tubing was pressed

through the other end of the channel. The overall device structure is illustrated in Fig. 5.

Branched and linear microfluidic devices were designed to create the 2-D and 3-D DIB networks respectively. Both these devices had ultra-microbore polytetrafluoroethylene (PTFE) 400 μm inner diameter (ID) inlet tubing delivering the microdroplets and microbore PTFE 800 μm ID outlet tubing carrying the waste product (both purchased from Cole-Parmer, UK). The outlet tubings were connected *via* 1 ml plastic syringes (InkjetF, B.Braun, Germany) to a dual-head syringe pump (Harvard 33 Twin Syringe Pump, Harvard Apparatus). The pump was set to refill mode and provided the pressure to direct the formation of the different network architectures.

No surface treatment was made to the PDMS channels as the lipid-in approach for DIB formation was employed. Fresh devices were used for each experiment. In the future, for experiments where proteins would be introduced and where surface chemistry may be of greater importance, surface modification of the devices may become necessary.

Conclusion

This work outlines novel microfluidic methods which are able to form extensive DIB networks in an automated, controlled and high-throughput manner. The branched device allowed DIB networks to be generated according to the contours of a microfluidic chip for the first time. This generic methodology can be extended and adapted to form other types and network geometries. The linear channel device enabled the formation of multiple 2-D and 3-D interconnected, multi-contact DIB networks, directed by external parameters without the need to change the device specifications. The ability to dial up networks of varying user-defined connectivities is a particularly powerful feature. Although the above experiments focus on droplets of differing lipid composition, the methodologies could equally be extended to incorporate droplets carrying different protein/drug/reagents within them. In both devices, control of droplet position and composition of individual droplets within the 2-D networks was achieved leading to defined patterned arrays of different bilayer lipid compositions, including asymmetric membranes. To exert finer positional control over individual droplets, particularly in the 3-D arrays, optical trapping techniques could be deployed.[18–20]

The development of artificial cells and organelles which mimic key functions and properties of biology will lead to new approaches for personalized healthcare, smart delivery systems, basic components for biological computing devices and the manufacture of organic compounds. Such systems must incorporate directed information flow and material transport and compartmentalised reactors with defined spatial connectivity, key features of their *in vivo* counterparts. Engineering these features into artificial cells and organelles requires being able to link together membrane compartments of defined shapes and sizes with controlled levels of asymmetry over long length scales. The ability to construct long range 3-D DIB networks opens up the possibility of constructing such assemblies which can eventually incorporate complex cellular communication and signalling network mimics.

Acknowledgements

This work was supported by EPSRC Grants EP/G00465X/1, EP/H024425/1, BBSRC Grant BB/F013167/1 and by an EPSRC Centre for Doctoral Training Studentship from the Institute of Chemical Biology (Imperial College London) awarded to YE.

References

1 H. Bayley, B. Cronin, A. J. Heron, M. A. Holden, W. L. Hwang, R. Syeda, J. Thompson and M. Wallace, *Mol. BioSyst.*, 2008, **4**, 1191.
2 S. A. Sarles and D. J. Leo, *Lab Chip*, 2010, **10**, 710–717.
3 W. L. Hwang, M. Chen, B. D. Cronin, M. A. Holden and H. Bayley, *J. Am. Chem. Soc.*, 2008, **130**, 5878–5879.
4 W. L. Hwang, M. A. Holden, S. White and H. Bayley, *J. Am. Chem. Soc.*, 2007, **129**, 11854–11864.
5 M. A. Holden, D. Needham and H. Bayley, *J. Am. Chem. Soc.*, 2007, **129**, 8650–8655.
6 G. Maglia, A. J. Heron, W. L. Hwang, M. A. Holden, E. Mikhailova, Q. Li, S. Cheley and H. Bayley, *Nat. Nanotechnol.*, 2009, **4**, 437–440.
7 G. Villar, A. J. Heron and H. Bayley, *Nat. Nanotechnol.*, 2011, **6**, 803–808.
8 C. E. Stanley, K. S. Elvira, X. Z. Niu, A. D. Gee, O. Ces, J. B. Edel and A. J. deMello, *Chem. Commun.*, 2010, **46**, 1620.
9 K. Funakoshi, H. Suzuki and S. Takeuchi, *Anal. Chem.*, 2006, **78**, 8169–8174.
10 S. Aghdaei, M. E. Sandison, M. Zagnoni, N. G. Green and H. Morgan, *Lab Chip*, 2008, **8**, 1617–1620.
11 J. Poulos, *Appl. Phys. Lett.*, 2009, **95**, 013706.
12 N. Malmstadt, M. A. Nash, R. F. Purnell and J. J. Schmidt, *Nano Lett.*, 2006, **6**, 1961–1965.
13 D. B. Weibel, *Curr. Opin. Chem. Biol.*, 2006, **10**, 584.
14 Y. C. Tan, J. S. Fisher, A. I. Lee, V. Cristini and A. P. Lee, *Lab Chip*, 2004, **4**, 292.
15 R. R. Pompano, *Annu. Rev. Anal. Chem.*, 2011, **4**, 59.
16 L. Shui, *Soft Matter*, 2009, **5**, 2708.
17 Y. Bai, X. He, D. Liu, S. N. Patil, D. Bratton, A. Huebner, F. Hollfelder, C. Abell and W. T. S. Huck, *Lab Chip*, 2010, **10**, 1281.
18 R. M. Lorenz, J. S. Edgar, G. D. M. Jeffries and D. T. Chiu, *Anal. Chem.*, 2006, **78**, 6433–6439.
19 A. E. Carruthers, J. P. Reid and A. J. Orr-Ewing, *Opt. Express*, 2010, **18**, 14238–14244.
20 D. R. Burnham and D. McGloin, *Opt. Express*, 2006, **14**, 4176–4182.

